Three Genes of the Arabidopsis *RPP1* Complex Resistance Locus Recognize Distinct *Peronospora parasitica* Avirulence Determinants

Miguel A. Botella,[a,1] Jane E. Parker,[a] Louise N. Frost,[a] Peter D. Bittner-Eddy,[b] Jim L. Beynon,[b] Michael J. Daniels,[a] Eric B. Holub,[b] and Jonathan D. G. Jones[a,2]

[a] Sainsbury Laboratory, John Innes Centre, Colney Lane, Norwich, NR4 7UH, United Kingdom
[b] Horticulture Research International, Wellesbourne, Warwickshire, CV35 9EF, United Kingdom

Plant resistance (*R*) genes have evolved specific recognition capabilities in defense against pathogens. The evolution of *R* gene function and maintenance of *R* gene diversity within a plant species are therefore of great interest. In the Arabidopsis accession Wassilewskija, the *RPP1* region on chromosome 3 contains four genetically linked recognition specificities, conditioning resistance to different isolates of the biotrophic oomycete *Peronospora parasitica* (downy mildew). We show that three of four tightly linked genes in this region, designated *RPP1-WsA*, *RPP1-WsB*, and *RPP1-WsC*, encode functional products of the NBS-LRR (nucleotide binding site–leucine-rich repeat) R protein class. They possess a TIR (Toll, interleukin-1, resistance) domain that is characteristic of certain other NBS-LRR–type R proteins, but in addition, they have unique hydrophilic or hydrophobic N termini. Together, the three *RPP1* genes account for the spectrum of resistance previously assigned to the *RPP1* region and thus comprise a complex *R* locus. The distinct but partially overlapping resistance capabilities conferred by these genes are best explained by the hypothesis that each recognizes a different pathogen avirulence determinant. We present evidence suggesting that the *RPP* genes at this locus are subject to the same selective forces that have been demonstrated for structurally different LRR-type *R* genes.

INTRODUCTION

Genotype-specific disease resistance in plants depends on the expression of complementary avirulence (*Avr*) genes in the pathogen and resistance (*R*) genes in the host (Staskawicz et al., 1995; Bent, 1996). The final outcome of a matched *R–Avr* interaction is incompatibility, that is, containment of the pathogen at the site of penetration, and is commonly associated with a hypersensitive response of the penetrated host cells. The underlying biochemical mechanism of this process and the continuing evolution of both *R* and *Avr* genes are therefore of great interest in plant pathology. The evolution of *R* genes in Arabidopsis is the focus of the work described here.

Characterization of a number of pathogen *Avr* genes suggests that some are derived from pathogenicity (or virulence) determinants that have become vulnerable to detection by a "surveillance system" in plants specified by evolving *R* genes and coupled in some way to rapid defense activation

(Baker et al., 1997). A powerful selection pressure is therefore exerted on the pathogen to mutate from avirulence to virulence, as has been demonstrated in several fungal (Joosten et al., 1994; Rohe et al., 1995) and bacterial (Kearney et al., 1988; Bogdanove et al., 1998) plant pathogens. It is crucial that the host plant is able to respond by generating novel recognition capabilities.

Pathogen "recognition" is thought to be the first step in disease resistance that serves as a signal for a general defense response. Plant *R* genes are therefore envisaged as encoding receptor proteins that specifically bind the cognate Avr protein ligand. Yeast two-hybrid analysis suggested a direct interaction between the tomato *PTO* gene product, which is a serine/threonine protein kinase, and *AvrPto* from *Pseudomonas syringae* pv *tomato* (Scofield et al., 1996; Tang et al., 1996). However, the majority of cloned *R* genes encode proteins that are not kinases; rather, they possess variable numbers of leucine-rich repeats (LRRs; Jones and Jones, 1997). Several recent reports suggest that the LRR motif permits the recurrent generation of novel protein–protein recognition specificities. This can occur through hypervariability in predicted solvent-exposed amino acids in a putative parallel β-sheet recognition surface and/or through variation in LRR copy number (Parniske et al., 1997;

Thomas et al., 1997). Structural comparisons between the tomato Cf-9 and Cf-4 R proteins revealed significant sequence divergence only within the N-terminal portion of their LRRs, implicating this domain in specific Avr recognition (Thomas et al., 1997). Molecular analysis of allelic variants at the flax *L* locus also suggests that the LRR domain is partly responsible for recognitional specificity (Ellis et al., 1997). The nature of repeated LRR sequence blocks in the Arabidopsis RPP5 protein further suggests that these have arisen through intragenic duplications (Parker et al., 1997). Thus, LRR domains are amenable to expansion and contraction by insertion or deletion of complete LRR units, potentially giving rise to novel recognition surfaces.

The majority of *R* genes reside at complex loci, and the structure of these may influence the rate of *R* gene diversification (Pryor and Ellis, 1993). The maize *Rp1* locus (Sudupak et al., 1993), the tomato *Cf-4/9* locus (Parniske et al., 1997; Thomas et al., 1997), the flax *M* locus (Anderson et al., 1997), and the lettuce *Dm3* locus (Anderson et al., 1996) all consist of genetically linked resistance specificities. Furthermore, *Rp1* gene instability and the creation of novel resistance specificities were shown to be associated with the exchange of flanking markers (Sudupak et al., 1993; Richter et al., 1995), suggesting that unequal crossing over contributes to sequence variation at *R* gene loci. Molecular analysis of genes comprising the *Cf-4/9* locus in tomato revealed a number of distinct *R* gene specificities (Parniske et al., 1997). Here, evidence was presented for diversifying selection within the LRRs on amino acids that are predicted to be solvent exposed and therefore may mediate ligand binding.

Extensive genetic variation exists in the interaction between the model plant, Arabidopsis, and the biotrophic oomycete *Peronospora parasitica* (downy mildew), indicative of a highly coevolved pathosystem (reviewed in Holub and Beynon, 1997). More than 20 downy mildew resistance specificities have been mapped to *RPP* (for recognition of *P. parasitica*) loci on six of the 10 chromosome arms of Arabidopsis by using differential responses of four standard accessions to a diverse collection of *P. parasitica* isolates. Although clustering of *RPP* loci has been observed in linkage groups of up to 15 centimorgans (cM), often coinciding with additional LRR-containing genes (Botella et al., 1997; M.G.M. Aarts et al., 1998), an example of a complex locus, such as those described in crop species (genetic scale <1 cM) conferring multiple resistance specificities, has yet to be clearly demonstrated in Arabidopsis.

Three downy mildew specificities (*RPP1*, *RPP10*, and *RPP14*), which previously were mapped to the same locus on the bottom arm of chromosome 3, were the focus of our effort to identify a complex locus of multiple specificities in Arabidopsis. *RPP1* was characterized first as a specificity in accession Niederzenz (Nd-1), conferring resistance to the *P. parasitica* isolate Emoy2 (Holub et al., 1994; Tör et al., 1994). In accession Wassilewskija (Ws-0), resistance to Emoy2 was inseparable by genetic recombination from the *RPP1* locus identified in Nd-1 (Holub et al., 1994; Holub and Beynon,

1997), suggesting that an *RPP1* allele exists in Ws-0. *RPP10* was designated as a second specificity in Ws-0, conferring resistance to the Nd-1–compatible *P. parasitica* isolate Cala2. Although *RPP10* has not been separated by genetic recombination from *RPP1*-Emoy2 in Ws-0, a mutation affecting resistance to Cala2 (Ws-0 *rpp10*) was identified, confirming that Ws-0 carried at least two downy mildew resistance genes at the *RPP1/10* locus (Holub, 1997). *RPP14* was designated as a third specificity to explain resistance in Ws-0 to an Nd-1–compatible isolate, Noco2 (Reignault et al., 1996). This isolate remains incompatible in the Ws-0 *rpp10* mutant, suggesting that either a third Noco2-specific gene exists in Ws-0 at the *RPP1/10/14* locus or that the *RPP1-Nd* and *RPP1-Ws* alleles defined by Emoy2 have different specificities as defined by Noco2.

The focus of our current investigation has been to test our hypothesis that Ws-0 carries more than one gene at the *RPP1/10/14* locus to explain the specificities predicted by using the three *P. parasitica* isolates Emoy2, Cala2, and Noco2. A new isolate, Maks9, was also included in this analysis. Resistance to this latter isolate maps to the same locus (Holub, 1997). We show that *RPP1/10/14* is indeed a complex locus that carries at least three functional genes that differ in their ability to detect the four *P. parasitica* isolates. The genes encode Toll–interleukin-1–resistance (TIR)—nucleotide binding site (NBS)—LRR proteins with closely related sequences. However, their distinct resistance profiles lead us to conclude that they must recognize different pathogen *Avr* genes or alleles. One of the R proteins contains an N-terminal putative signal anchor, resembling L6. The other two proteins lack the signal anchor, but both encode a novel and unique hydrophilic N terminus. We also present evidence suggesting that positive selection for diversification of the predicted ligand binding domain has affected the evolution of the *RPP1* gene family.

RESULTS

### High-Resolution Mapping of *RPP14*

The *RPP14* specificity in Ws-0 was chosen as the first target for positional cloning by using the corresponding *P. parasitica* isolate Noco2 to characterize recombinants from a cross between Ws-0 and the Noco2-compatible accession Columbia (Col-0). *RPP14* was previously mapped to a 3.2-cM interval between the restriction fragment length polymorphism (RFLP) markers ve021 (centromeric) and pAT3-89.1 (telomeric) on chromosome 3 (Reignault et al., 1996). The flanking markers were used to identify yeast artificial chromosome (YAC) clones from the available Arabidopsis CIC YAC library containing DNA inserts derived from Col-0 (Creusot et al., 1995; Botella et al., 1997). These YAC clones were oriented relative to each other and the RFLP markers,

revealing a maximum physical interval of 800 kb between the two flanking RFLP markers, as shown in Figure 1A. The position of the *RPP14* locus in Col-0 was further delimited by positioning two YAC-derived end probes on recombinant plants (see Methods) and using the end probes to identify overlapping P1 clones (Liu et al., 1995; Figure 1B). EcoRI restriction fragments from the clones P1-37C7 and P1-53P2 were cloned and sequenced. One of the subclones (37C7-5; Figure 1B) derived from P1-37C7 contained an open reading frame with similarity to the LRR region of *RPP5* (Parker et al., 1997), although no hybridization was detected in the YAC encompassing the Col-0 *RPP14* region when *RPP5* was used in low-stringency hybridization (data not shown). Based on this homology, we considered it likely that the 37C7-5 sequence was part of an *rpp14* allele in Col-0.

Gel blot analysis of DNA from several Arabidopsis accessions, using the Col-0 37C7-5 fragment as a probe, showed the presence of a highly polymorphic multigene family (Figure 1C). All polymorphic family members cosegregated as two separate groups corresponding with phenotypic classes of the two parental accessions, Ws-0 or Col-0. In addition, all Col-0 hybridizing bands were contained on YAC clones CIC6B1 and CIC8D7, indicating that they spanned a maximum physical distance of ~400 kb, which is the distance encompassed by the YAC clones. Three or four gene members were found in all accessions analyzed, with the exception of Nd-1, which appears to contain a more complex gene family (Figure 1C). Most importantly, molecular evidence for a gene family in Ws-0 suggested that it should be possible to determine which genes may explain the *RPP1*, *RPP10*, and *RPP14* specificities.

Isolation of *RPP1/10/14* Gene Candidates from Ws-0

Clones from a binary vector cosmid library (Arabidopsis Biological Resource Center, Columbus, OH) containing Ws-0 genomic DNA were identified using the 37C7-5 Col-0 DNA probe and assembled into two contigs, as shown in Figure 2A. Two members of the gene family were identified in this library, including homolog A (*Hom-A*) contained in cosmid ws-cos65.1 and *Hom-B* contained in cosmid ws-cos69.12. A third family member, *Hom-C* (contained in phage 1.1), was identified by screening a Ws-0 genomic DNA phage library (Dietrich et al., 1997). A 1.1-kb HindIII DNA fragment from ws-cos65.1 was identified that distinguished between the different gene copies (Figure 2A). Gel blot analysis of DNA from Arabidopsis accessions Ws-0 and Col-0, using this probe, revealed four hybridizing bands (Figure 2B). Therefore, we conclude that there is a fourth member of the gene family, designated *Hom-D*. However, no cosmid or phage clones were identified that contained this homolog. The EcoRI and HindIII fragment patterns deduced from the sequence of the Ws-0 candidate genes correspond to the hybridizing fragments assigned to *Hom-A*, *Hom-B*, and *Hom-C* in Figure 2B.
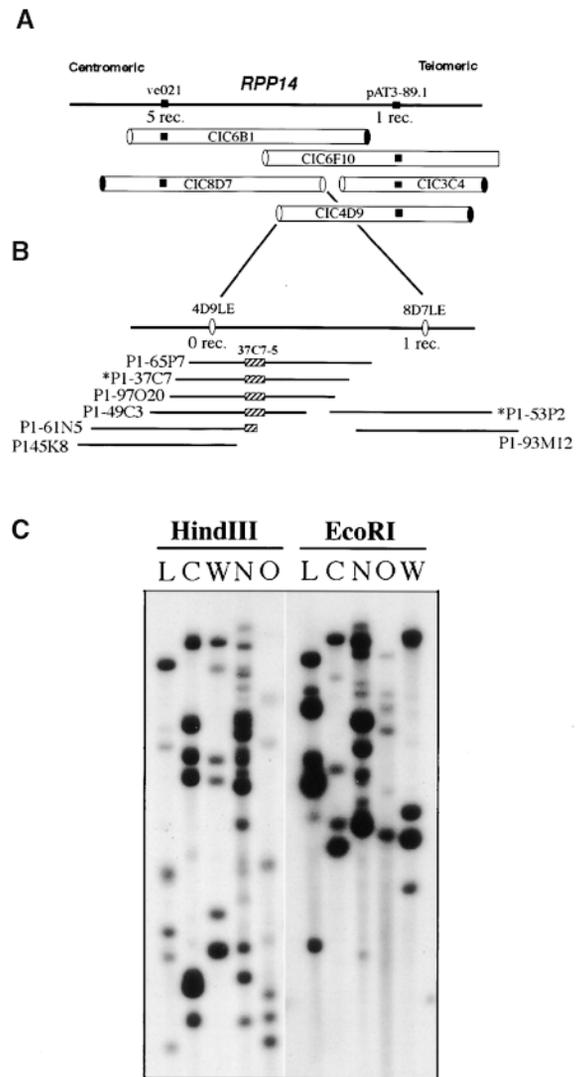

Figure 1. Physical Delineation of *RPP14.*

(A) Alignment of YAC clones relative to molecular markers flanking *RPP14.* Individual YAC clones were positioned by hybridization with the RFLP flanking markers ve021 and pAT3-89.1. End probes from the YACs (solid ellipses for the right ends and open ellipses for the left ends) were obtained as described in Methods and used to orient the YAC clones.

(B) Two YAC end probes, 4D9LE and 8D7LE, were used to isolate overlapping P1 clones. Two of the P1 clones, P1-37C7 and P1-53P2, which are marked with asterisks, were found to overlap. Random sequence of these clones identified a fragment, 37C7-5 (striped boxes), with homology to *RPP5.*

(C) DNA gel blot analysis of five Arabidopsis accessions reveals a small, polymorphic gene family. The blot was hybridized at high stringency and probed with the 37C7-5 fragment. DNA from the accessions Landsberg *erecta* (L), Col-0 (C), Ws-0 (W), Nd-1 (N), and Oystese (O) were digested with EcoRI and HindIII as indicated.
rec., recombinant.

A

B
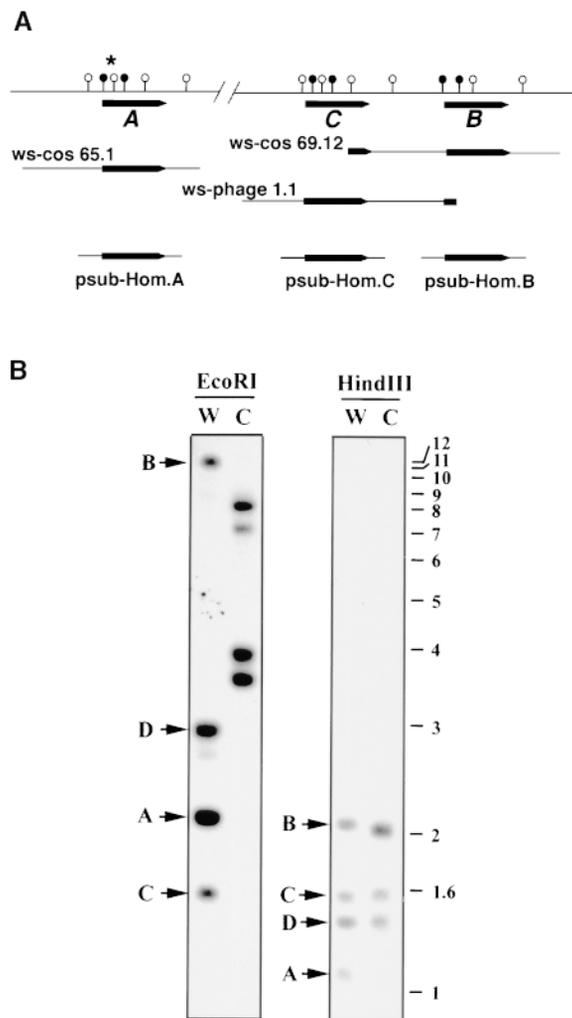
Figure 2. Physical Organization of *RPP1/10/14* Candidate Genes in Ws-0.

(A) Three different genes containing 37C7-5–homologous sequence were identified and assembled into two contigs. Only informative clones are shown. Minimal constructs for *Hom-A* (psub-Hom.A), *Hom-B* (psub-Hom.B), and *Hom-C* (psub-Hom.C) were derived from ws-cos65.1, ws-cos69.12, and ws-phage1.1 (see Methods). EcoRI restriction sites are indicated by open circles and HindIII sites by filled circles. The 1.1-kb HindIII probe from the 5′ end of *Hom-A* that was used in the DNA gel blot analysis shown in **(B)** is indicated with an asterisk. Thick black arrows represent positions of the genes (from ATG to stop codon).

(B) DNA from the Ws-0 (W) and Col-0 (C) Arabidopsis accessions was digested with HindIII or EcoRI. The filter was probed with a 1.1-kb HindIII fragment from the 5′ end of *Hom-A*. The identity of fragments derived from the *Hom-A*, *Hom-B*, and *Hom-C* genes is indicated at left. Molecular markers are indicated at right. Hybridizing bands derived from *Hom-D* are also shown.

Determining the Functions of *Hom-A*, *Hom-B*, and *Hom-C*

The Noco2-compatible accession Col-0 was not suitable for transgenic experiments to determine the function of the three homologs because it is incompatible with the *P. parasitica* isolates Cala2 and Emoy2, which are recognized, respectively, by *RPP2* and *RPP4* on chromosome 4. Therefore, we selected a plant line from the Col-0 × Ws-0 mapping cross that was homozygous for the disease-sensitive alleles from Ws-0 at *RPP2* and *RPP4* and from Col-0 at *RPP1/10/14* by using polymerase chain reaction (PCR)–based markers that defined these regions on each chromosome. We confirmed that progeny from this line were uniformly susceptible to isolates Noco2, Emoy2, and Cala2 as well as to a fourth Ws-0–incompatible isolate Maks9 (data not shown). The susceptible line is denoted CW84 and was used as a recipient for Agrobacterium-mediated transformation with each of the candidate genes.

Stable transformants (T_1 plants) of CW84 were obtained with binary cosmid clone ws-cos65.1 (*Hom-A*; Figure 2A) and Ws-0 genomic DNA fragments containing only *Hom-A*, *Hom-B*, or *Hom-C* that had been cloned into the binary vector pSLJ755I5 (see Methods). Selfed T_2 progeny and homozygous T_3 progeny of several independent transformants for each construct were inoculated with each of the Ws-incompatible *P. parasitica* isolates (Table 1). *Hom-A* conferred resistance on all four isolates; *Hom-B* conferred partial resistance (see below) to the isolates Noco2, Emoy2, and Maks9 but was fully susceptible to Cala2; and *Hom-C* specified resistance only to Noco2. All transgenic lines were also tested against Emco5 (Table 1), an isolate that is compatible in both Ws-0 and Col-0, thus confirming that the transgenes were specific only to the Ws-0–incompatible isolates. Resistance in Ws-0 to isolates Noco2, Emoy2, and Cala2 is known to require another component encoded by the *EDS1* (for enhanced disease susceptibility) gene (Parker et al., 1996; N. Aarts et al., 1998). Analysis of F_2 progeny from a cross between a CW84 line containing multiple copies of *Hom-A* and a Ws-0 *eds1* mutant line, *eds1-1*, showed that *EDS1* also was necessary for the function of this transgene (Table 1).

The response phenotypes of wild-type Ws-0, CW84, and CW84 transgenic lines containing *Hom-A*, *Hom-B*, or *Hom-C* after inoculation with isolate Noco2 are shown in Figure 3. As in leaves of wild-type Ws-0 (Figure 3A), *Hom-A* conferred effective resistance on Noco2 in transgenic CW84 (Figure 3B). Asexual sporulation was never observed in leaves after inoculations of either transgenic Hom-A or wild-type resistant plants. A similar phenotype with no sporulation was observed in transgenic Hom-A plants inoculated with isolates Emoy2, Maks9, and Cala2 (data not shown). Resistance specified by *Hom-C* to Noco2 appeared to be as strong in transgenic CW84 as in CW84 lines containing *Hom-A* (data not shown). In contrast, *Hom-B* conferred only partial resistance to Noco2 (Figure 3C), Emoy2, and Maks9, allowing sparse asexual sporulation of all three isolates. Neverthe-

Table 1. Interaction Phenotypes of Different Wild-Type, Transgenic, and Mutant Arabidopsis Accessions after Inoculations with Five Isolates of *P. parasitica*

Arabidopsis Line	No. of Lines Analyzed	No. of Resistant Lines to the Following *P. parasitica* Isolates				
		Noco2	Emoy2	Cala2	Maks9	Emco5
Ws-0	1	1	1	1	1	0
Col-0	1	0	1	1	NT[a]	0
CW84	1	0	0	0	0	0
Ws-0 *rpp10*	1	1	1	0	NT	NT
CW84[b]						
ws-cos65.1	6	6	6	6	6	0
psub–Hom-A	12	11	11	11	11	0
psub–Hom-B[c]	12	12	12	0	12	0
psub–Hom-C	12	12	0	0	0[d]	0
CW84–*Hom-A* × eds1 F₂[e]	2	0	0	0	NT	0

[a] NT, not tested.

[b] The constructs used for transformation are shown in Figure 2A. The complete cosmid ws-cos65.1 was used in the transformation.

[c] The interaction phenotypes in most of these lines were characterized by a low level of *P. parasitica* sporulation.

[d] Only four lines were tested for the interaction phenotype.

[e] A Ws-0 *eds1* mutant was used in the cross (Parker et al., 1996).

less, sporulation was markedly less compared with heavy sporulation observed on nontransformed CW84 (Figure 3D). The different resistance phenotypes were confirmed by microscopic examination of inoculated leaves that had been stained with lactophenol trypan blue (Reignault et al., 1996). In leaves of Ws-0 and transgenic Hom-A plants, hyphal growth was restricted to a few host cells, as shown for Noco2 (Figures 3E and 3F). Hyphal growth extended further in transgenic Hom-B leaves, but this was associated with necrosis of penetrated host cells (Figure 3G) and was not as extensive as pathogen development in nontransformed CW84 (Figure 3H). Col-0 was transformed with either *Hom-A* or *Hom-B*, and these transgenic plants produced the response phenotypes to Noco2, as was observed in CW84 (data not shown), indicating that the different phenotypic expressions of *Hom-A* and *Hom-B* were not a consequence of the recombinant background of CW84.

The pathology data demonstrated that three members of the gene family are functional downy mildew resistance genes and that each exhibits a unique specificity for recognizing different combinations of *P. parasitica* isolates. Hereafter, we refer to each of the functional homologs as *RPP1-WsA*, *RPP1-WsB*, and *RPP1-WsC* for *Hom-A*, *Hom-B*, and *Hom-C*, respectively. This nomenclature will be useful for designating functional homologs from other accessions, such as one or more expected from Nd-1 (P.D. Bittner-Eddy, E.B. Holub, and J.L. Beynon, unpublished data). We will denote the locus and family of genes, regardless of accession, as the *RPP1* complex locus and the *RPP1* gene family.

DNA Structure of Three Functional Genes within the *RPP1* Complex Locus

A 2.8-kb EcoRI fragment from *RPP1-WsA* was used as a probe to isolate cDNAs from a Ws-0 silique cDNA library, and several partial cDNAs were characterized (see Methods) to confirm the location of introns within the three functional genes. Their structure and organization are shown in Figure 4A. The positions of intron–exon splice junctions are conserved in all three genes, except at the 5′ termini. Here, two additional introns were identified in the *RPP1-WsB* and *RPP1-WsC* alleles, one located in the 5′ untranslated region and the second 181 bp (*RPP1-WsB*) and 169 bp (*RPP1-WsC*) downstream from their predicted start codons.

The Predicted Protein Products of the *RPP1* Gene Family

These three genes encode similarly sized proteins of 1189, 1221, and 1217 amino acids, respectively, that possess a high overall identity (Figure 4B). Comparison of their predicted amino acid sequences with GenBank database sequences showed that they are most similar to the products encoded by *RPP5* (Parker et al., 1997), *N* (Whitham et al., 1994), and *L6* (Lawrence et al., 1995), which are all functional R proteins containing an NBS and C-terminal LRRs. This affiliation includes N-terminal similarity to the cytoplasmic domains of the *Drosophila* Toll and mammalian interleukin-1 receptor, the so-called TIR domain (Figure 4B; see also
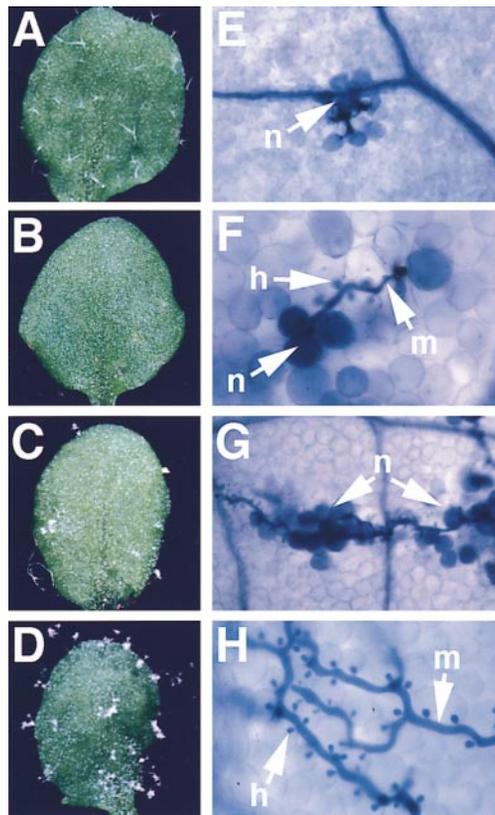
Figure 3. Response Phenotypes of Arabidopsis Leaves 6 Days after Inoculation with *P. parasitica* Isolate Noco2.

Nine-day-old seedlings were spray inoculated with a suspension of conidiosporangia. The phenotypes were monitored macroscopically with a hand lens and microscopically by observing lactophenol try-pan blue–stained leaves. h, haustorium; m, mycelium; n, necrotic plant cell.

(A) and **(E)** Resistance in wild-type Ws-0 specified by *RPP14*. Noco2 mycelium is effectively contained within a discrete cluster of plant necrotic cells at the site of attempted penetration.

(B) and **(F)** Resistance in a CW84 line that is homozygous for T-DNA containing the minimal *Hom-A* construct (see Figure 2A). Resistance is as effective as in wild-type Ws-0.

(C) and **(G)** Resistance in a CW84 line that is homozygous for T-DNA carrying *Hom-B* (see Figure 2A) is less effective than is wild-type Ws-0. A low level of pathogen asexual sporulation is visible, and lim-ited mycelium development was accompanied by a trail of necrotic plant cells.

(D) and **(H)** High levels of pathogen asexual sporulation are visible in the broadly compatible line CW84. Extensive mycelium growth and haustorial development occurred in the absence of plant cell necrosis.

Figure 5). Like RPP5, N, and L6, the kinase-1a (P loop; GPPGIGKTT), kinase-2 (FLVLDE), and kinase-3a (FGPGSR) consensus motifs that constitute a predicted NBS (Traut, 1994) are contained entirely within RPP1-WsA, RPP1-WsB, and RPP1-WsC (Figure 4). The spacing between these three

motifs is consistent with that found in known ATP and GTP binding proteins (Traut, 1994).

The C-terminal portion of the RPP1 family of proteins can be divided into two regions (Figures 4B and 6). The first is composed of imperfect LRRs conforming to the canonical LRR consensus for cytoplasmic LRR proteins (Jones and Jones, 1997). As in other TIR-NB-LRR products, a cysteine residue is frequently found in the β-turn region after the
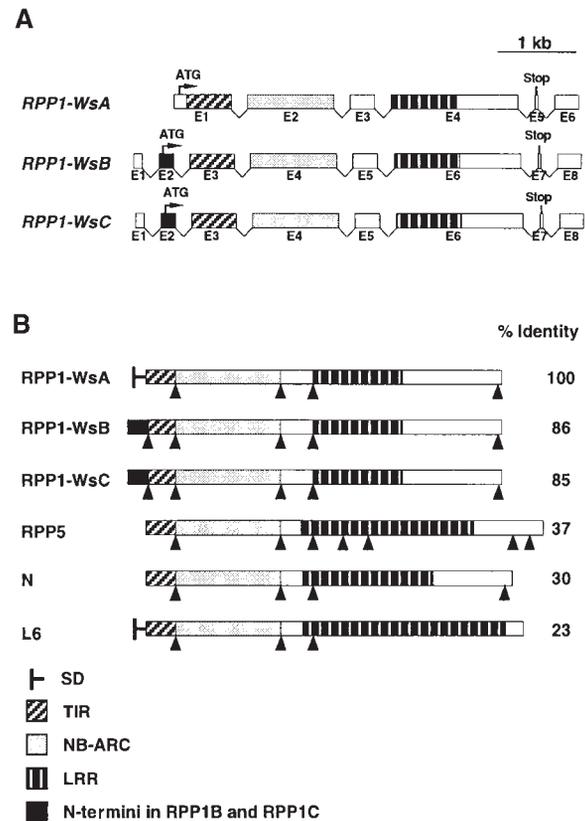
Figure 4. Structure of the *RPP1* Gene Family Members and Their Predicted Proteins.

(A) Sequence features of genes *RPP1-WsA*, *RPP1-WsB*, and *RPP1-WsC*. E1 to E8 represent exons 1 to 8. The predicted ATG and the stop codons are shown. Exons showing high homology are indi-cated with symbols as given in the key.

(B) Schematic comparison of the RPP1 protein family of related *R* gene products. The percentage of amino acid sequence identity be-tween RPP1-WsA and RPP1-WsB, RPP1-WsC, RPP5, N, and L6 is shown. Intron positions are marked by arrowheads. Similar protein domains are indicated with identical shading according to the key. The TIR domain has similarity with the cytoplasmic domains of Toll and IL-1R (see also Figure 5). The NB-ARC domain contains motifs that constitute an NBS and domains with homology to APAF-1 and CED-4, regulators of cell death. LRR corresponds to the C-terminal part of the proteins that contain the LRRs. N termini correspond to the extension of the proteins observed in RPP1-WsB and RPP1-WsC. Signal domain (SD) is observed in RPP1-WsA and L6.

A

B

Figure 5. Alignment and Hydrophobicity Plot of the TIR Domains of RPP1-WsA, RPP1-WsB, RPP1-WsC, RPP5, N, and L6.

(A) Prettybox representation of a Pileup analysis (Genetics Computer Group, Madison, WI) of the TIR region of RPP1-WsA (exon 1), RPP1-WsB (exons 1 and 2), RPP1-WsC (exons 1 and 2), RPP5 (exon 1), N (exon 1), and L6 (exon 1). The N-terminal extensions of the RPP1 family and L6 proteins relative to RPP5 and N are shaded and indicated by an arrow. The asterisk indicates the position of the introns in RPP1-WsB and RPP1-WsC. Black boxes indicate identity and gray boxes similarity. Dashes are gaps introduced by the program to optimize the alignment.
(B) Hydrophobicity analysis of the sequences shown in **(A)**. The N-terminal extensions are shaded and indicated by an arrow. Analysis was performed as detailed in Methods.

LXXLXLXX motif, where X stands for any amino acid (Jones and Jones, 1997). Ten LRRs varying in length from 21 to 24 amino acids were identified in RPP1-WsA and RPP1-WsB, and nine LRRs were identified in RPP1-WsC (Figure 6). The second part in the C terminus does not contain LRRs, and the proportion of leucine residues is only 12% compared with 22% in the LRR region.

The most striking differences in the predicted proteins were found at their N termini (Figures 4B and 5A). A hydrophobic domain, predicted to be a membrane anchor (Von

Heijne, 1986), was located in the RPP1-WsA protein that extends its N terminus by 40 amino acids relative to RPP5 and N. An N-terminal signal peptide has also been predicted for the L6 protein (Lawrence et al., 1995), although no sequence homology was found in this domain between RPP1-WsA and L6 (Figure 5A). An additional exon in RPP1-WsB and RPP1-WsC (Figures 4B and 5A) extended the N-terminal ends of the encoded proteins into a strong hydrophilic region beyond the TIR domain (Figure 5B). A BLAST search using the first exon of RPP1-WsB and RPP1-WsC did not

A

TIR

```
                                        ↓
MDSSFFLVLVAAATGFFMLFRKFRFHQDNKESNSSSLSRPTAATSVSRNW
KHDVFPSFHGADVRRTFLSHILESFRRKGIDTFIDNNIERSKSIGPELKE
AIKGSKIAIVLLSRKYASSSWCLDELAEIMKCREVLGQIVMTIFYEVEPT
DIKKQTGEFGKAFTKTCRGKTKEHIERWRKALEDVATIAGYHSHKW·
```

NB-ARC

```
SNEAEMIEKISTDVSNMLDLSIPSKDFDDFVGMAAHMERTEQLLRLDLDE
ARMIGIWGPPGIGKTTIARFLFNQVSDRFQLSAIMVNIKGCYPRPCFDEY
SAQLQLQNQMLSQMINHKDIMISHLGVAQERLRDKKVFLVLDEVDQLGQL
DALAKDTRWFGPGSRIIITTEDQGILKAHGINHVYKVEYPSNDEAFQIFC
MNAFGQKQPYEGFCDLAWEVKALAGELPLGLKVLGSALRGMSKPEWERTL
PRLRTSLDGKIGGIIQFSYDALCDEDKYLFLYIACLFNNESTTKVEEVLA
NKFLDVGQGIHVLAQKSLISFEGEEIQMHTLLEQFGRETSRKQFVHHRYT
KHQLLVGERDICEVLNDDT·
```

```
IDSRRFIGIHLDLSKNEEELNISEKALERIHDFQFVRINDKNHALHERLQ
DLICHSPKISLKWYSYQNICLPSTFNPEFLVELDMSFSKLQKLWEGTKQL
·R
```

LRRs

```
NL KWMDLSY SSYLKELPNLSTAT
NL EELNLRN CSSLVELPSSIEKLT
SL QILDLQG CSSLVELPSFGNAT
KL EILYLDY CRSLEKLPPSINAN
NL QKLSLRN CSRIVELPAIENAT
NL WELNLLN CSSLIELPLSIGTARNL
FL KELNISG CSSLVKLPSSIGDMT
NL KEFDLSN CSNLVELPSSIGNLQ
NL CKLIMRG CSKLEALPININLK
SL DTLNLTD CSQLKSFPEISTHIK
```

```
YLRLTGTAIKEVPLSIMSWSPLAEFQISYFESLKEFPHAFDIITELQLSH
DIQEVTPWVKRMSRLRYFRLNNCNNLVSLPQLPDSLAYLYADNCKSLEKL
DCCFNNPWISLHFPKCFKLNQEARDLIMHTSTSRIAMLPGTQVPACFNHR
ATSGDYLKIKLKESPLPTTLRFKACIMLVMVNEGISYDRKIKLSVDIRDE
QNDLKVQCTPSGCYIYPLTEHIYTFELEVEEVTSTELVFEFTLDKESNWK
IGECGILQRETRSLRRSSSPDLPSESSR·
```

```
VSSYNHC
```

B

	RPP1Ws-A vs RPP1Ws-B	RPP1Ws-A vs RPP1Ws-C	RPP1Ws-B vs RPP1Ws-C
xx(L)x(L)xx	20/50 (40%)	17/45 (37%)	19/45 (42%)
nonframed	9/189 (5%)	15/182 (8%)	11/190 (6%)

C

	synonymous	nonsynonymous
xx(L)x(L)xx	9.3±3.9	25.2±3.3
nonframed	5.4±1.2	3.5±0.8
complete gene	7.9±1.0	7.2±0.4

Figure 6. Structural Domains of the RPP1 Protein Family and Analysis of Their LRRs.

(A) The RPP1 family of proteins can be divided into several domains. The TIR domain (exon 1 in RPP1-WsA, RPP5, N, and L6; exon 2 and exon 3 in RPP1-WsB and RPP1-WsC) is similar to the cytoplasmic domains of Drosophila Toll and mammalian interleukin-1 receptors. The NB-ARC domain (exon 2 in RPP1-WsA, RPP5, N, and L6; exon 4 in RPP1-WsB and RPP1-WsC) has similarity to the nematode CED-4 and mammalian APAF-1 proteins, which are both activators of apoptotic proteases (Van der Biezen and Jones, 1998).

reveal significant homology in the database, and its role is unclear.

Identification of Mutant Alleles at the *RPP1* Complex Locus

Ws-0 seedlings derived from ethyl methanesulfonate–mutagenized M_2 seeds and the Feldmann Ws-0 T-DNA–tagged lines (see Methods) were inoculated with Noco2, Emoy2, or Cala2 and screened for mutations from disease resistance to susceptibility. No mutations to Noco2 and Emoy2 were found that mapped to the *RPP1* complex locus. This can be explained by the presence of more than one gene conferring resistance to those isolates (Table 1). However, a mutant line, Ws-0 *rpp10*, that had lost resistance to Cala2 but retained the wild-type resistance response to Noco2 and Emoy2 was identified (Table 1). Analysis of F_2 progeny derived from backcrossing the mutant with Ws-0 showed that the recessive mutant phenotype did not cosegregate with the presence of the T-DNA. The mutation was shown to be linked to the morphological glabrous marker *gl-1*, which is tightly linked to the *RPP1/10/14* locus. Based on complementation analysis of the wild-type *RPP1* homologs (Holub, 1997; Table 1), we anticipated that this mutant should contain a defective allele of *RPP1-WsA*. Sequence analysis of

The LRR domain (exons 3 to 6 in RPP5; exons 3 and 4 in N and L6; exon 4 in RPP1-WsA; and exon 6 in RPP1-WsB) is envisaged to mediate specific protein–protein interactions. Residues corresponding to the β-strand/β-turn structural motif in the porcine ribonuclease inhibitor are delimited by vertical lines in the RPP1-WsA sequence. Identical amino acids between RPP1-WsA, RPP1-WsB, and RPP1-WsC are shown in black. Amino acids conserved in only two of the proteins are shown in blue. Different amino acids in all three proteins are shown in red. The conserved kinase-1a (P loop) domain (GPPGIGKTT), the kinase-2 domain (FLVLDE), the kinase-3a domain (FGPGSR), and the hydrophobic motif conserved in this class of proteins (ELPLGL) are underlined. An 11–amino acid deletion in the Ws-*rpp10* mutant is highlighted by the upper box within the NB-ARC domain. A deletion of one LRR in RPP1-WsC LRR is highlighted by the lower boxes. The arrow in the TIR domain indicates the start of homology among the RPP1-WsA, RPP1-WsB, and RPP1-WsC proteins.
(B) Amino acid differences within the LRR domains between the RPP1 family of proteins. The number of different amino acids, the number of amino acids used, and the percentage of difference are indicated. Amino acids changes are more prevalent in the predicted β-strand/β-turn structural motif that is predicted to interact with the cognate ligand (Jones and Jones, 1997).
(C) Synonymous and nonsynonymous nucleotide substitutions in different regions of the coding sequences of the *RPP1* gene family. The values shown are calculated as described previously (Parniske et al., 1997).

RPP1-WsA in the mutant revealed the presence of an in-frame deletion of 33 nucleotides encoding 11 amino acids in the NBS domain (Figure 6A) that precede a hydrophobic amino acid motif highly conserved in NBS-LRR resistance proteins (Parker et al., 1997; Hammond-Kosack and Jones, 1997). We have therefore designated this Ws-0 mutant as *rpp1-WsA.*

Variation among *RPP1* Gene Family Members in Nonsynonymous Nucleotide Substitutions Encoding the Solvent-Exposed Residues of the LRRs

The LRR domain is proposed to confer recognition specificity of ligand binding due to its capacity to evolve new configurations by deletion, insertions, and nucleotide substitutions (Jones and Jones, 1997; Parniske et al., 1997). For example, a deletion of a complete LRR was found in RPP1-WsC compared with RPP1-WsA and RPP1-WsB (Figure 6). Further comparison of amino acid differences in the LRRs among RPP1-WsA, RPP1-WsB, and RPP1-WsC from Ws-0 showed that most changes are found in the residues predicted to be solvent exposed (37 to 42%), whereas only 5 to 8% take place in the rest of the LRR domain (Figure 6B). Interestingly, in the LRR domain, it is only in solvent-exposed positions that amino acid substitutions in all three proteins are found.

Comparison of synonymous (K_s) and nonsynonymous (K_a) substitution rates per synonymous/nonsynonymous site can be used to determine the type of selection acting on a gene family. When the K_a/K_s ratio is 1 or similar, a ratio that has been observed in pseudogenes, no selection pressure is operating (Hughes, 1995). A K_a/K_s ratio >1 suggests that diversifying selection has influenced the evolution of the gene family (Hughes and Nei, 1988; Parniske et al., 1997). The rates of synonymous and nonsynonymous nucleotide substitutions among members of the *RPP1* gene family were calculated for the XX(L)X(L)XX sequence of the LRRs, the nonconsensus amino acids of which are predicted to be solvent exposed (Kobe and Deisenhofer, 1993, 1994; Parniske et al., 1997; Thomas et al., 1997). The rate of nonsynonymous substitutions (K_a) in this region was more than seven times higher than that observed in other regions of the protein. However, the rate of synonymous substitutions was found to be similar (Figure 6C). The value for the K_a/K_s ratio in the XX(L)X(L)XX region is >1, suggesting that positive selection for diversification in the predicted ligand binding domain has affected the evolution of the *RPP1* gene family.

DISCUSSION

At least three Arabidopsis *RPP* specificities to *P. parasitica* isolates Emoy2 (*RPP1*), Cala2 (*RPP10*), and Noco2 (*RPP14*) are closely linked on the long arm of chromosome 3 in ac-

cession Ws-0 (Holub et al., 1994; Reignault et al., 1996). In this study, we have cloned and assigned a recognition function to three out of four genes that belong to a physically tightly linked *R* gene family. The resistance phenotypes conferred by these three genes can account for the three *RPP* specificities identified in this region, though we have not yet defined the function(s) of *Hom-D.* The isolation and characterization of the *RPP1* gene family now permit detailed analysis of the molecular mechanisms underpinning parasite recognition and the selective forces directing the evolution of novel recognition specificities at a complex *R* gene locus in Arabidopsis.

Three *RPP1* Gene Family Members Have Distinct but Overlapping Functions

The recognition specificities conferred by the three *RPP* genes cloned and individually analyzed in this study were distinguished using four Ws-0–incompatible *P. parasitica* isolates (Table 1). All three genes (*RPP1-WsA*, *RPP1-WsB*, and *RPP1-WsC*) conferred resistance to Noco2, two genes conferred resistance to Emoy2 and Maks9 (*RPP1-WsA* and *RPP1-WsB*), and only one gene (*RPP1-WsA*) specified resistance to Cala2. These results suggest that the RPP1-WsA protein recognizes an Avr determinant that is common to all four isolates. Thus, RPP1-WsB is likely to be interacting with a different Avr determinant that is present in Noco2, Emoy2, and Maks9 but absent from Cala2. Similarly, RPP1-WsC must be recognizing an Avr determinant that is unique to Noco2. Because the genes at the *RPP1* locus are very similar and have probably evolved from a common ancestor, and because *P. parasitica* is diploid, it is possible that they recognize different but related (allelic) Avr determinants. However, it is also possible that they recognize unrelated Avr determinants, as in the case of *RPM1* or *Cf-4* and *Cf-9* (Grant et al., 1995; Thomas et al., 1997). Therefore, including *RPP5*, it is likely that *RPP* genes that recognize four different *Avr* gene products of Noco2 are now in hand.

Differences among *RPP1-WsA*, *RPP1-WsB*, and *RPP1-WsC* Resistance Phenotypes

Interestingly, *RPP1-WsA* and *RPP1-WsC* conferred a strong resistance, whereas *RPP1-WsB* specified only partial resistance. Although the different recognition specificities conferred by *RPP1-WsA*, *RPP1-WsB*, and *RPP1-WsC* indicate genetic variation among *Avr* genes in the parasite isolates used in this study, the phenotype of the *R* gene–mediated response is also likely to be influenced by a number of other factors. R and Avr protein expression levels, the timing of *Avr* gene expression during pathogen development, the zygotic condition of alleles at *Avr* loci (*P. parasitica* is a diploid organism), and the efficiency of delivery of the parasite's Avr or compatibility signals to the plant could all affect the

phenotype. Future experiments will test whether the difference in interaction phenotypes is correlated with expression of the respective R proteins. *RPP* gene dosage was shown previously to influence the interaction phenotype, and it was possible to discriminate phenotypically between plants homozygous or heterozygous at the *RPP14* (Reignault et al., 1996) and *RPP5* (Parker et al., 1993) loci.

Predicted Functional Domains of the RPP1 Proteins

The three *RPP1* gene family members identified and characterized here add to the set of predicted NBS-LRR proteins that have been assigned recognition function in plant disease resistance (Bent, 1996). These proteins possess the structural attributes that would fulfill two anticipated functions: recognition specificity with potential for adaptive variability within the LRRs (see also below) and conserved motifs that may direct transduction of common signals in the defense response.

Highest RPP1 amino acid sequence conservation was observed with RPP5, N, and L6 over the TIR domain (Figures 5B and 6). Therefore, RPP1-WsA, RPP1-WsB, and RPP1-WsC can be considered to belong to the TIR-NBS-LRR subclass of NBS-LRR proteins that possesses N-terminal similarity to Toll and the interleukin-1 receptor (Hammond-Kosack and Jones, 1997). Members of this subclass that have been characterized in Arabidopsis are dependent on a second gene, *EDS1*, for resistance function (N. Aarts et al., 1998). An unexpected observation was the presence of additional introns at the 5′ end of the *RPP1* and *RPP14* genes that give rise to hydrophilic N-terminal extensions beyond the TIR domain and the N termini of the predicted RPP5, N, and L6 proteins (Figures 4 and 5). The role of these extensions is not clear, and no proteins with homology to these regions have been detected in the databases. Unlike RPP1 and RPP14, and like L6, RPP10 possesses an N-terminal extension of 40 amino acids relative to both RPP5 and N. This region is a potential signal anchor, suggesting that the protein may become membrane associated. Further studies are required to establish whether the differences in the respective N termini are reflected in different cellular locations. Whatever their role, they appear not to correlate with the strength of the resistance phenotypes observed here (Figure 3) or with a differential dependence on *EDS1*, because resistance to Noco2 was fully abolished in a Ws-0 *eds1* background (Parker et al., 1996).

It is predicted that the NBS domain binds ATP or GTP as part of a conserved and essential feature of pathogen recognition specified by the NBS-LRR R protein class. Like other NBS-LRR R proteins, RPP1 proteins carry extended homology to APAF-1 and CED-4, regulators of cell death in animal cells (Van der Biezen and Jones, 1998). It is postulated that this region, designated the NB-ARC domain by Van der Biezen and Jones (1998), may serve an adapter function that transduces information from an LRR-modu-

lated recognition event to a common signaling element such as the TIR domain.

Evolutionary Forces Operating at the *RPP1* Locus

Complex *R* loci are widespread in Arabidopsis and other plant species. The tomato *Cf-4/9* locus and the tomato *Pto* locus contain multiple genes, most of which are functional (Jia et al., 1997; Parniske et al., 1997). In contrast, the rice *Xa21* locus and the Arabidopsis *RPP5* locus from Col-0 are also multicopy but contain a high proportion of pseudogenes (Song et al., 1997; Bevan et al., 1998). These are thought to have arisen by an initial tandem duplication followed by unequal crossing-over events (Holub, 1997; Hulbert, 1997). Evolutionary novelty at *R* gene loci has been correlated with meiotic events that involve either crossovers or gene conversions (Hulbert, 1997; Parniske et al., 1997).

Molecular analysis of three out of four genes comprising the *RPP1* complex locus points to at least two tandem duplications followed by sequence divergence giving rise to *Hom-A* to *Hom-D*. Duplicated functional genes may provide several selective advantages. Their arrangement could allow multiple specificities to be assembled and retained in a single haplotype, thus preserving the potential for variation and the evolution of novel specificities through mispairing, intergenic recombination, and gene duplication (Parniske et al., 1997; Thomas et al., 1997). Such mechanisms would be expected to rapidly generate novel gene variants. The higher number of homologous *RPP1* sequences present in the Nd-1 accession (Figure 1C) probably indicates a locus-dependent and intraspecific copy number expansion. Genetic and RFLP analyses in Nd-1 demonstrated that all polymorphic bands mapped to the same location as the members of the Ws-0 *RPP1* locus (data not shown). The presence of functional genes at the *RPP1* complex locus can be assumed to be a result of an active selection pressure from the pathogen. *RPP1-WsA*, *RPP1-WsB*, and *RPP1-WsC* all recognize Noco2, and this redundancy would allow diversification of one of the genes by relaxing the selection pressure on the remaining genes in the complex. If, as we surmise, the *RPP* genes in the cluster recognize different Avr determinants, their presence would provide a clear selective advantage against pathogen variants that have lost individual *Avr* genes through mutation. There is evidence that sequence exchange has taken place between different *RPP1* genes of Ws-0 (data not shown). Shuffling of sequences is considered a major force in generating gene diversity. Indeed, DNA shuffling has been proven to be a powerful process for directed evolution by recombination to combine useful variation from homologous genes (Crameri et al., 1998).

It is envisaged that the LRR domain confers specificity in pathogen recognition due to its capacity to evolve new configurations (Jones and Jones, 1997). Analysis of several alleles from the *L* locus and chimeric genes in flax supports this view (Ellis et al., 1997). Two key mechanisms are pro-

posed to create sequence diversity within the LRRs. In the first, deletion or insertion of complete LRRs may occur by intragenic crossing over. This was revealed in a mutant allele of *RPP5* that has an in-frame intragenic duplication of four LRRs without loss of function (Parker et al., 1997). In the second, an enhanced rate of nonsynonymous nucleotide substitutions in the solvent-exposed residues of the LRRs appears to operate, as shown for members of the *Cf-4/9* locus (Jones and Jones, 1997; Parniske et al., 1997). Evidence for both mechanisms was observed in the three genes of the *RPP1* complex. Deletion of a complete LRR was found in RPP1-WsC (Figure 6). Deletion of a different LRR was also observed in a Col-0 *rpp1* allele (M.A. Botella, unpublished data).

We observed a high degree of sequence variation in the interstitial amino acid residues that are predicted to be solvent exposed in the LRR β-strand/β-turn region, based on the structure of the porcine ribonuclease inhibitor (Kobe and Deisenhofer, 1995). Within the genes of the *RPP1* complex locus, the high degree of polymorphism observed in those residues supports a role for these sequences in recognition specificity, as was shown previously for genes of the tomato *Cf-4/9* complex. Here, we present evidence that sequence diversity is positively selected for (as indicated by a high K_a/K_s ratio), in a region predicted to be involved in specificity. In contrast, the remainder of the protein exhibits a K_a/K_s ratio of ~1. We conclude that evolution of the LRRs in different structural classes of *R* gene product from different plant species has been brought about by very similar mechanisms and selective forces.

METHODS

Cultivation of *Arabidopsis thaliana* Plants and Pathogenicity Tests

The origins of Columbia (Col-0) and Wassilewskija (Ws-0) were as reported by Reignault et al. (1996). Col-0 × Ws-0 F_2 seed was used for the mapping of *RPP14.* The Ws-*rpp10* mutant line was selected from the K. Feldmann T-DNA lines (Feldmann, 1992). The conditions for plant cultivation, maintenance of *Peronospora parasitica,* and pathogenicity tests were as described previously (Holub et al., 1994; Parker et al., 1997).

Analysis of Recombinants

Analysis of 90 F_2 seedlings (or corresponding F_3 families) generated from a cross between Col-*glabrous* (*gl*) and Ws-0 and 48 F_2 seedlings generated from a cross between Col-*gl* and Pr-0 showed linkage of *RPP14* to the marker *Gl-1* on chromosome 3. The Col-*gl* × Ws-0 and Col-*gl* × Pr-0 populations were considered together in our efforts to clone *RPP14* because an allelism test between Ws-0 and Pr-0 showed a complete cosegregation between the two resistance loci (Reignault et al., 1996).

Plant Genomic DNA Preparations

Large-scale plant genomic DNA preparations and rapid, small-scale DNA samples were made as described previously (Parker et al., 1993; Reignault et al., 1996). The method of Klimyuk et al. (1993) was used to prepare denatured DNA suitable for polymerase chain reaction (PCR) amplification.

DNA Manipulations

A binary Ws-0 library (Arabidopsis Biological Resource Center) and phage Ws-0 genomic libraries (a kind gift of J. Dangl, University of North Carolina, Chapel Hill) were screened using the 37C7-5 probe. Three binary cosmid clones were obtained that contained homolog A (*Hom-A*), and two cosmid clones were obtained that contained *Hom-B*. A genomic phage (1.1) was obtained containing *Hom-C*. Cosmid subclones were inserted into the binary cosmid vector pSLJ755I5 (http://www.uea.ac.uk/nrp/jic/s3d_plas.htm) and cultured in the presence of 50 mg/L tetracycline. P1 clones were cultured in the presence of 50 mg/L kanamycin. DNA of these clones was obtained using the alkaline lysis method (Liu et al., 1995). Fingerprinting of cosmids and P1 clones was performed by digesting the DNA with several restriction enzymes, end labeling with phosphorus-33, and separating the fragments on a sequencing gel. Several partial cDNAs were identified in a Ws-0 cDNA library derived from Arabidopsis siliques (Castle and Meinke, 1994; Arabidopsis Biological Resource Center) by using a 2.8-kb EcoRI probe from *Hom-A* (see Figure 2A).

Yeast Artificial Chromosome DNA Manipulations

Yeast artificial chromosome (YAC) clones from the CIC library (Creusot et al., 1995) were identified as described previously (Botella et al., 1997). Left end or right end YAC DNA probes were generated by inverse PCR using YAC vector nested primers, as described previously (Schmidt and Dean, 1995), or thermal-asymmetric-interlaced (TAIL)–PCR (Liu et al., 1995). The end probes derived from the YAC clones were agarose gel purified and then used to probe plant genomic DNA blots. YACs were oriented relative to each other by probing YAC ends with filters containing YAC clone DNA.

Sequence Analysis

A shotgun cloning approach was used to determine the nucleotide sequence of the three genes. *Escherichia coli* DH5α transformants harboring recombinant clones containing Arabidopsis DNA subcloned in pUC18 were identified by hybridization with insert DNA isolated from the cosmids ws-cos65.1, ws-cos69.12, and phage 1.1 (Figure 2A). M13 universal forward and reverse primers were used to determine end sequences by using the dye deoxy terminator cycle sequencing method (Applied Biosystems [ABI], La Jolla, CA) and an ABI model 377 sequencing system. Sequence contigs were assembled using UNIX versions of the Staden programs package (Roger Staden, MRC, Cambridge, UK). Computer-aided sequence similarity searches were made with BLAST (Altschul et al., 1990) programs and the National Center for Biotechnology Information (Bethesda, MD) nucleotide and peptide sequence databases. Secondary structure predictions and determination of signal peptides were made with the predict programs (http://www.cmpharm.ucsf.edu/~nomi/nnpredict.html and http://cookie.imcb.osaka-u.ac.jp/nakai/psort.html). The accession

numbers for *RPP1-WsA*, *RPP1-WsB*, and *RPP1-WsC* are AF098962, AF098963, and AF098964, respectively.

Construction of Subclones Containing *Hom-A*, *Hom-B*, and *Hom-C*

All subclones containing members of the *RPP1* gene family were constructed in the binary vector pSLJ755I5. For psub–Hom-A, a 7-kb DNA fragment originating from partial SpeI digestion of the ws-cos65.1 clone was subcloned into pUC118. A KpnI fragment obtained from *Hom-A* from a KpnI site located 2.7 kb upstream of the predicted ATG translation start codon and the KpnI site of the pUC118 polylinker was subcloned into the KpnI site of the pOK12 vector (Vieira and Messing, 1991). The SpeI fragment liberated from the vector was subcloned into the compatible XbaI site of pSLJ755I5. For psub–Hom-B, an 11-kb Pst fragment derived from ws-cos69.12 was subcloned into the PstI site of the binary vector. For psub–Hom-C, a SalI-SpeI fragment and a SpeI-EcoRI fragment derived from phage 1.1 were subcloned into the XhoI-EcoRI site of the binary vector by using a three-way ligation.

Arabidopsis Transformation

The whole-plant infiltration method of Bechtold et al. (1993) was used for the transformation experiments. Transformed (T$_1$) seedlings were selected on Arabidopsis medium (Bechtold et al., 1993) containing 50 mg/L hygromycin for selection of ws-cos65.1 transformants. For all the constructs made using the pSLJ755I5 vector, transformed (T$_1$) seedlings were selected by spraying L-phosphinothricin at 100 mg/L on young seedlings.

REFERENCES

Aarts, M.G.M., te Lintel Hekkert, B., Holub, E.B., Beynon, J.L., Stiekema, W.J., and Pereira, A. (1998). Identification of *R*-gene homologous DNA fragments genetically linked to disease resistance loci in *Arabidopsis thaliana*. Mol. Plant Microbe Interact. **11**, 251–258.

Aarts, N., Metz, M., Holub, E.B., Staskawicz, B.J., Daniels, M.J., and Parker, J.E. (1998). Different requirements for *EDS1* and *NDR1* by disease resistance genes define at least two *R* gene–mediated pathways in *Arabidopsis*. Proc. Natl. Acad. Sci. USA **95**, 10306–10311.

Altschul, S.F., Gish, W., Miller, W., Meyers, E.W., and Lipman, D.J. (1990). Basic local alignment search tool. J. Mol. Biol. **215**, 403–410.

Anderson, P.A., Arroyogarcia, R., Meyers, B.C., and Michelmore, R.W. (1996). Molecular analysis of irradiation-induced and spontaneous deletion mutants at a disease resistance locus in *Lactuca sativa*. Mol. Gen. Genet. **251**, 316–325.

Anderson, P.A., Lawrence, G.J., Morrish, B.C., Ayliffe, M.A., Finnegan, E.J., and Ellis, J.G. (1997). Inactivation of the flax resistance gene *M* associated with loss of a repeated unit within the leucine-rich repeat coding region. Plant Cell **9**, 641–651.

Baker, B., Zambryski, P., Staskawicz, B., and Dinesh-Kumar, S.P. (1997). Signaling in plant–microbe interactions. Science **276**, 726–733.

Bechtold, N., Ellis, J., and Pelletier, G. (1993). In planta *Agrabacterium*-mediated gene transfer by infiltration of adult *Arabidopsis thaliana* plants. C.R. Acad. Sci. Ser. III Sci. Vie **316**, 1194–1199.

Bent, A.F. (1996). Plant disease resistance genes: Function meets structure. Plant Cell **8**, 1757–1771.

Bevan, M., et al. (1998). Analysis of 1.9 Mb of contiguous sequence from chromosome 4 of *Arabidopsis thaliana*. Nature **391**, 485–488.

Bogdanove, A.J., Kim, J.F., Wei, Z.M., Kolchinsky, P., Charkowski, A.O., Conlin, A.K., Collmer, A., and Beer, S.V. (1998). Homology and functional similarity of an *hrp*-linked pathogenicity locus, *dspEF*, of *Erwinia amylovora* and the avirulence locus *avrE* of *Pseudomonas syringae* pathovar *tomato*. Proc. Natl. Acad. Sci. USA **95**, 1325–1330.

Botella, M.A., Coleman, M.J., Hughes, D.E., Nishimura, M.T., Jones, J.D.G., and Somerville, S.C. (1997). Map positions of 47 Arabidopsis sequences with sequence similarity to disease resistance. Plant J. **12**, 1197–1211.

Castle, L.A., and Meinke, D.W. (1994). A *FUSCA* gene of Arabidopsis encodes a novel protein essential for plant development. Plant Cell **6**, 25–41.

Crameri, A., Raillard, S.A., Bermudez, E., and Stemmer, W.P.C. (1998). DNA shuffling of a family of genes from diverse species accelerates directed evolution. Nature **391**, 288–291.

Creusot, F., Fouilloux, E., Dron, M., Lafleuriel, J., Picard, G., Billault, A., Lepaslier, D., Cohen, D., Chaboute, M.E., Durr, A., Fleck, J., Gigot, C., Camilleri, C., Bellini, C., Caboche, M., and Bouchez, D. (1995). The CIC library—A large insert YAC library for genome mapping in *Arabidopsis thaliana*. Plant J. **8**, 763–770.

Dietrich, R.A., Richberg, M.H., Schmidt, R., Dean, C., and Dangl, J.L. (1997). A novel zinc finger protein is encoded by the Arabidopsis *LSD1* gene and functions as a negative regulator of plant cell death. Cell **88**, 685–694.

Ellis, J., Lawrence, G., Ayliffe, M., Anderson, P., Collins, N., Finnegan, J., Frost, D., Luck, J., and Pryor, T. (1997). Advances in the molecular genetic analysis of the flax–flax rust interaction. Annu. Rev. Phytopathol. **35**, 271–291.

Feldmann, K.A. (1992). T-DNA insertion mutagenesis in *Arabidopsis*: Mutational spectrum. Plant J. **1**, 71–82.

Grant, M.R., Godiard, L., Straube, E., Ashfield, T., Lewald, J., Sattler, A., Innes, R.W., and Dangl, J.L. (1995). Structure of the *Arabidopsis RPM1* gene enabling dual specificity disease resistance. Science **269**, 843–846.

Hammond-Kosack, K.E., and Jones, J. (1997). Plant disease resistance genes. Annu. Rev. Plant Physiol. Plant Mol. Biol. **48**, 575–607.

Holub, E.B. (1997). Organization of resistance genes in Arabidopsis. In The Gene-for-Gene Relationship in Plant–Parasite Interactions, I.R. Crute, E.B. Holub, and J.J. Burdon, eds (Wallingford, UK: CAB International), pp. 5–26.

Holub, E.B., and Beynon, J.L. (1997). Symbiology of mouse-ear cress (*Arabidopsis thaliana*) and oomycetes. Adv. Bot. Res. **24**, 227–273.

Holub, E.B., Beynon, J.L., and Crute, I.R. (1994). Phenotypic and genotypic characterization of interactions between isolates of *Peronospora parasitica* and accessions of *Arabidopsis thaliana*. Mol. Plant-Microbe Interact. **7**, 223–239.

Hughes, A.L. (1995). Origin and evolution of *Hla* class-I pseudogenes. Mol. Biol. Evol. **12**, 247–258.

Hughes, A.L., and Nei, M. (1988). Pattern of nucleotide substitution at major histocompatibility complex class-I loci reveals overdominant selection. Nature **335**, 167–170.

Hulbert, S.H. (1997). Structure and evolution of the *rp1* complex conferring rust resistance in maize. Annu. Rev. Phytopathol. **35**, 293–310.

Jia, Y., Loh, Y.-T., Zhou, J., and Martin, G.B. (1997). Alleles of *Pto* and *Fen* occur in bacterial speck-susceptible and fenthion-insensitive tomato cultivars and encode active protein kinases. Plant Cell **9**, 61–73.

Jones, D.A., and Jones, J.D.G. (1997). The roles of leucine-rich-repeat proteins in plant defenses. Adv. Bot. Res. **24**, 89–167.

Joosten, M.H.A.J., Cozijnsen, T.J., and De Wit, P.J.G.M. (1994). Host resistance to a fungal tomato pathogen lost by a single base-pair change in an avirulence gene. Nature **367**, 384–386.

Kearney, B., Ronald, P.C., Dahlbeck, D., and Staskawicz, B.J. (1988). Molecular basis for evasion of plant host defence in bacterial spot disease of pepper. Nature **332**, 541–543.

Klimyuk, V.I., Carroll, B.J., Thomas, C.M., and Jones, J.D.G. (1993). Alkali treatment for rapid preparation of plant tissue for reliable PCR analysis. Plant J. **3**, 493–494.

Kobe, B., and Deisenhofer, J. (1993). Crystal structure of a porcine ribonuclease inhibitor, a protein with leucine-rich repeats. Nature **366**, 751–756.

Kobe, B., and Deisenhofer, J. (1994). The leucine-rich repeat: A versatile binding motif. Trends Biochem. Sci. **19**, 415–421.

Kobe, B., and Deisenhofer, J. (1995). Proteins with leucine-rich repeats. Curr. Opin. Struct. Biol. **5**, 409–416.

Lawrence, G.J., Finnegan, E.J., Ayliffe, M.A., and Ellis, J.G. (1995). The *L6* gene for flax rust resistance is related to the Arabidopsis bacterial resistance gene *RPS2* and the tobacco viral resistance gene *N*. Plant Cell **7**, 1195–1206.

Liu, Y.G., Mitsukawa, N., Vazqueztello, A., and Whittier, R.F. (1995). Generation of a high-quality P1 library of Arabidopsis suitable for chromosome walking. Plant J. **7**, 351–358.

Parker, J.E., Szabo, V., Staskawicz, B.J., Lister, C., Dean, C., Daniels, M., and Jones, J.D.G. (1993). Phenotypic characterization and molecular mapping of the *Arabidopsis thaliana* locus *RPP5*, determining resistance to *Peronospora parasitica*. Plant J. **4**, 821–831.

Parker, J.E., Holub, E.B., Frost, L.N., Falk, A., Gunn, N.D., and Daniels, M.J. (1996). Characterization of *eds1*, a mutation in Arabidopsis suppressing resistance to *Peronospora parasitica* specified by several different *RPP* genes. Plant Cell **8**, 2033–2046.

Parker, J.E., Coleman, M.J., Szabò, V., Frost, L.N., Schmidt, R., van der Biezen, E.A., Moores, T., Dean, C., Daniels, M.J., and Jones, J.D.G. (1997). The Arabidopsis downy mildew resistance gene *RPP5* shares similarity to the Toll and interleukin-1 receptors with *N* and *L6*. Plant Cell **9**, 879–894.

Parniske, M., Hammond-Kosack, K.E., Golstein, C., Thomas, C.M., Jones, D.A., Harrison, K., Wulff, B.B.H., and Jones, J.D.G. (1997). Novel disease resistance specificities result from sequence exchange between tandemly repeated genes at the *Cf-4/9* locus of tomato. Cell **91**, 821–832.

Pryor, T., and Ellis, J. (1993). The genetic complexity of fungal resistance genes in plants. Adv. Plant Pathol. **10**, 281–305.

Reignault, P., Frost, L.N., Richardson, H., Daniels, M.J., Jones, J.D.G., and Parker, J.E. (1996). Four *Arabidopsis RPP* loci controlling resistance to the Noco2 isolate of *Peronospora parasitica* map to regions known to contain other *RPP* recognition specificities. Mol. Plant-Microbe Interact. **9**, 464–473.

Richter, T.E., Pryor, T.J., Bennetzen, J.L., and Hulbert, S.H. (1995). New rust resistance specificities associated with recombination in the *Rp1* complex in maize. Genetics **141**, 373–381.

Rohe, M., Gierlich, A., Hermann, H., Hahn, M., Schmidt, B., Rosahl, S., and Knogge, W. (1995). The race-specific elicitor, Nip1, from the barley pathogen, *Rhynchosporium secalis*, determines avirulence on host plants of the *rrs1* resistance genotype. EMBO J. **14**, 4168–4177.

Schmidt, R., and Dean, C. (1995). Hybridization analysis of YAC clones. Methods Mol. Cell. Biol. **5**, 309–318.

Scofield, S.R., Tobias, C.M., Rathjen, J.P., Chang, J.F., Lavelle, D.T., Michelmore, R.W., and Staskawicz, B.J. (1996). Molecular basis of gene-for-gene specificity in bacterial speck disease of tomato. Science **274**, 2063–2065.

Song, W.-Y., Pi, L.-Y., Wang, G.-L., Gardner, J., Holsten, T., and Ronald, P.C. (1997). Evolution of the rice *Xa21* disease resistance gene family. Plant Cell **9**, 1279–1287.

Staskawicz, B.J., Ausubel, F.M., Baker, B.J., Ellis, J.G., and Jones, J.D.G. (1995). Molecular genetics of plant disease resistance. Science **268**, 661–667.

Sudupak, M.A., Bennetzen, J.L., and Hulbert, S.H. (1993). Unequal exchange and meiotic instability of disease-resistance genes in the *Rp1* region of maize. Genetics **133**, 119–125.

Tang, X., Frederick, R.D., Zhou, J., Halterman, D.A., Jia, Y., and Martin, G.B. (1996). Physical interaction of AvrPto and the Pto kinase defines a recognition event involved in plant disease resistance. Science **274**, 2060–2063.

Thomas, C.M., Jones, D.A., Parniske, M., Harrison, K., Balint-Kurti, P.J., Hatzixanthis, K., and Jones, J.D.G. (1997). Characterization of the tomato *Cf-4* gene for resistance to *Cladosporium*

fulvum identifies sequences that determine recognitional specificity in Cf-4 and Cf-9. Plant Cell **9**, 2209–2224.

Tör, M., Holub, E.B., Brose, E., Musker, R., Gunn, N., Can, C., Crute, I.R., and Beynon, J.L. (1994). Map positions of three loci in *Arabidopsis thaliana* associated with isolate-specific recognition of *Peronospora parasitica* (downy mildew). Mol. Plant-Microbe Interact. **7**, 214–222.

Traut, T.W. (1994). The functions and consensus motifs of nine types of peptide segments that form different types of nucleotide-binding sites. Eur. J. Biochem. **229**, 9–19.

Van der Biezen, E.A., and Jones, J.D.G. (1998). The NB-ARC domain: A novel signaling motif shared by plant resistance gene products and regulators of cell death in animals. Curr. Biol. **8**, 226–227.

Vieira, J., and Messing, J. (1991). New pUC-derived cloning vectors with different selectable markers and DNA replication origins. Gene **100**, 189–194.

Von Heijne, G. (1986). A new method for predicting signal sequence cleavage sites. Nucleic Acids Res. **14**, 4683–4690.

Whitham, S., Dinesh-Kumar, S.P., Choi, D., Hehl, R., Corr, C., and Baker, B. (1994). The product of the tobacco mosaic virus resistance gene *N*: Similarity to Toll and the interleukin-1 receptor. Cell **78**, 1011–1115.

Three Genes of the Arabidopsis *RPP1* Complex Resistance Locus Recognize Distinct *Peronospora parasitica* Avirulence Determinants

Miguel A. Botella, Jane E. Parker, Louise N. Frost, Peter D. Bittner-Eddy, Jim L. Beynon, Michael J. Daniels, Eric B. Holub and Jonathan D. G. Jones

This information is current as of November 24, 2020

References	This article cites 52 articles, 18 of which can be accessed free at: /content/10/11/1847.full.html#ref-list-1
Permissions	https://www.copyright.com/ccc/openurl.do?sid=pd_hw1532298X&issn=1532298X&WT.mc_id=pd_hw1532298X
eTOCs	Sign up for eTOCs at: http://www.plantcell.org/cgi/alerts/ctmain
CiteTrack Alerts	Sign up for CiteTrack Alerts at: http://www.plantcell.org/cgi/alerts/ctmain
Subscription Information	Subscription Information for *The Plant Cell* and *Plant Physiology* is available at: http://www.aspb.org/publications/subscriptions.cfm